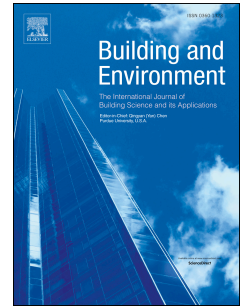


# Accepted Manuscript

Modeling of the aerosol infiltration characteristics in a cultural heritage building: The Baroque Library Hall in Prague

Sofia Eirini Chatoutsidou, Ludmila Mašková, Lucie Ondráčková, Jakub Ondráček, Mihalis Lazaridis, Jiří Smolík



PII: S0360-1323(15)00086-4

DOI: [10.1016/j.buildenv.2015.02.029](https://doi.org/10.1016/j.buildenv.2015.02.029)

Reference: BAE 4009

To appear in: *Building and Environment*

Received Date: 25 November 2014

Revised Date: 20 February 2015

Accepted Date: 21 February 2015

Please cite this article as: Chatoutsidou SE, Mašková L, Ondráčková L, Ondráček J, Lazaridis M, Smolík J, Modeling of the aerosol infiltration characteristics in a cultural heritage building: The Baroque Library Hall in Prague, *Building and Environment* (2015), doi: 10.1016/j.buildenv.2015.02.029.

This is a PDF file of an unedited manuscript that has been accepted for publication. As a service to our customers we are providing this early version of the manuscript. The manuscript will undergo copyediting, typesetting, and review of the resulting proof before it is published in its final form. Please note that during the production process errors may be discovered which could affect the content, and all legal disclaimers that apply to the journal pertain.

# Modeling of the aerosol infiltration characteristics in a cultural heritage building: The Baroque Library Hall in Prague

Sofia Eirini Chatoutsidou<sup>1,2\*</sup>, Ludmila Mašková<sup>3,4</sup>, Lucie Ondráčková<sup>3</sup>, Jakub Ondráček<sup>3</sup>,  
Mihalis Lazaridis<sup>2</sup> and Jiří Smolík<sup>3</sup>

<sup>1</sup>Norwegian Institute for Air Research (NILU), Instituttveien 18, 2007 Kjeller, Norway

<sup>2</sup>School of Environmental Engineering, Technical University of Crete, Polytechnioupolis, 73100 Chania, Greece

<sup>3</sup>Laboratory of Aerosol Chemistry and Physics, Institute of Chemical Process Fundamentals AS CR, Rozvojová 135, 165 02 Prague 6, Czech Republic

<sup>4</sup>Charles University in Prague, Faculty of Science, Institute of Environmental Studies, Benátská 2, 12 801 Prague 2, Czech Republic

*Keywords: infiltration factor, penetration, deposition, library, indoor sources*

## ABSTRACT

Three intensive campaigns in spring, summer and winter 2009 were conducted in the Baroque Library Hall in Prague, Czech Republic. The number concentration of particulate matter (PM) was measured online and simultaneously, both indoors and outdoors with an SMPS (0.014-0.7  $\mu\text{m}$ ) and an APS instrument (0.7-20  $\mu\text{m}$ ). A dynamic mass balance model was introduced taking account particle penetration from outdoors and indoor losses (deposition, ventilation). The model was used to determine deposition rate  $k$  and penetration efficiency  $P$  in 13 discrete size intervals. Model performance was evaluated using the coefficient of determination ( $R^2$ ) by selecting different pairs of  $k$  and  $P$ . No unique solution found, thus, averaged values of  $k$  and  $P$  from the best correlated pairs were used to estimate infiltration factor. Good agreement between infiltration factor and I/O ratio confirmed that modeled  $k$  and  $P$  were well-estimated. The deposition rate was found to depend strongly on particle size with higher rates for ultrafine and coarse particles. Penetration efficiency, on the other hand, was not clearly related with particle size. The infiltration factor varied substantially with particle size with less effective removal for accumulation fraction (0.1-0.7  $\mu\text{m}$ ). Higher infiltration factor for ultrafine particles, compared to coarse particles, indicates that enrichment of the library at this size is caused by penetration from outdoors. On the other hand, human presence during visiting hours found to contribute significantly to coarse particles by increasing the indoor number concentration by a factor of 3, 3.2 and 2 during spring, summer and winter respectively.

\*Address correspondence to Chatoutsidou Sofia Eirini, Norwegian Institute for Air Research (NILU), Instituttveien 18, 2007, Kjeller, Norway, Tel.: +47 6389 8167  
E-mail address: [SofiaIirini.Chatoutsidou@nilu.no](mailto:SofiaIirini.Chatoutsidou@nilu.no)

## 1. Introduction

Indoor air quality in cultural heritage buildings is a common issue in modern societies. Outdoor pollution changed considerably the last 50 years [1], thus, it is crucial to assess the impact of outdoor pollution to the indoor one, as well as indoor pollutants since they threaten the conservation and preservation of the collections [2].

Particulate matter can cause soiling by deposition and adsorption, material degradation or damage by chemical reactions [3-6]. Indoor pollutants in cultural heritage buildings may originate either from indoor sources or penetrate indoors through the building envelope [4,7-9]. Common indoor sources include heating, smoking, cleaning or walking. On the other hand, penetration depends on particle dynamics [10]. Particulate matter characteristics generated indoors are strongly connected with the primary indoor sources [11,12], whereas, particles that originate from outdoors are determined by building characteristics, ventilation, transport, particle dynamics and outdoor PM characteristics [10,13-17].

Numerous studies have already focused on indoor air characterization of libraries and museums with regard to chemical pollutants, indoor sources, chemical reactions and environmental factors [4,6-8,18-23,24]. Moreover, the characteristics of indoor PM in museums were also studied with regard to the outdoor environment [7,9,25,26]. These studies include buildings belonging to a complex or individuals, in suburban or urban areas, with natural or mechanical ventilation and different construction materials. In all cases, the results underline the influence of the indoor environment by the chemical composition of indoor pollutants, particulate matter concentration and the contribution from outdoor sources along with the impact from indoor human presence. Thus, the estimation of indoor pollutants originating from outdoors along with the impact from indoor sources became a crucial issue.

Penetration of outdoor particles indoors and building characteristics were studied thoroughly. The relationship of indoor and outdoor particulate matter was examined in several environments [27-32] and the reported results strongly associated the indoor PM concentration with the outdoor one. In respect to particle dynamics and using mass balance models, the authors managed to determine deposition indoors and penetration from outdoors, although the variability of the results indicated the strong dependence on assumptions, different methodologies and building characteristics [33-41]. However, all studies provided insight to particle dynamics indoors and associated both deposition and penetration with particle size.

The present study examined the particle number characteristics in Baroque Library Hall (BLH) in Prague, Czech Republic. A former study on indoor pollutants and indoor/outdoor pollutants relationship can be found in [22]. The BLH is a naturally ventilated building, which, along with the controlled access from the visitors, provided a sampling site appropriate for determining the infiltration of outdoor originated particles and investigation of the visitor's impact on indoor PM. The contribution of the present study is that it employs infiltration characteristics with size resolved analysis in a cultural heritage building as most of the studies in the topic involve domestic environments (houses). The objective was to evaluate particulate matter characteristics indoors with respect to outdoors, to estimate penetration of outdoor particles and deposition rates indoors using a dynamic mass balance model, to determine the infiltration factor and its dependence on particle size and finally to investigate the contribution of the visitors to the indoor particle concentration.

## **2. Experimental and methodology**

### **2.1 Sampling site**

The Baroque Library Hall of the National Library is part of Clementinum Historical Complex and is located in the Vltava River valley, right in the historical center of Prague. The intensity of car traffic in this area is approximately 24,200 cars per day [42]. Clementinum, built on an area of 2 hectares, is the second largest and the most historic complex of buildings in Prague. The Hall, situated in the center of the Clementinum on the second floor, holds approximately 20.000 theological books dating from the 16th century until recent times and stored in original wooden shelves.

Figure 1 presents the internal scheme of the library. It is 39 m long and 9.4 m wide with an arched ceiling in the lowest point at 8.3 m and in the highest point 9.5 m high. There are 8 double glass windows covered by curtains along the western and eastern side and 4 entrance doors, 2 on the north side and 2 on the south side. The doors on the north side lead from the hallway, which serves as a storage room and as entrance used by librarians and restorers. The doors on the south side lead from foyer of the Hall and serve as an entrance and exit for the visitors. The library is naturally ventilated with all windows closed, while, the doors open only for visiting purposes. The visitors enter the Hall in groups of maximum 25 people with the guide and run only along the south site of the Hall. Sightseeing tours took place every day from 10 am and started every half-hour during weekend and every hour during the rest of week. A detailed description of the library can be found in [43]. Any other activities (e.g. cleaning) in the indoor environment were very limited.

Figure 1: Scheme of the library and position of the instruments.

### **2.2 Measurement campaigns/Instrumentation**

The campaign was conducted during spring (10<sup>th</sup> - 17<sup>th</sup> March), summer (14<sup>th</sup> - 21<sup>th</sup> July) and winter (22<sup>th</sup> November - 2<sup>nd</sup> December) 2009. Indoor and outdoor particle number concentrations were measured by a Scanning Mobility Particle Sizer (SMPS, model 3934C, TSI, U.S.A.) consisted of a Differential Mobility Analyzer (DMA, model 3081), a Condensation Particle Counter (CPS, model 3775) and an Aerodynamic Particle Sizer (APS, model 3320, TSI, U.S.A.). Both instruments sampled from both inside and outside BLH simultaneously using its own sampling train provided with an electrically actuated three-way ball valve connected to a common programmable controller that used a CPC voltage (controlling the high voltage on the central rod of the DMA) as a signal for switching. The SMPS sampled with a flow rate at 0.3 l/min, measuring particle number concentration in the size range of 0.014-0.7  $\mu\text{m}$  in 110 channels. The APS was operated with 5 l/min flow rate and measured particles in the effective size range 0.7-20  $\mu\text{m}$  in 51 channels. The SMPS used 3 min upward scan, followed by one minute downward scan with one minute delay necessary to separate samples and wash sampling train after valve switching. Eventually two five-minute sampling cycles for indoor sampling followed by two five-minute cycles for outdoor sampling. The experimental set up of the instruments is shown in Figure 2. Data from both instruments were collected using Aerosol Instrument Manager software (AIM v.1.0, TSI, U.S.A.), where particle losses inside sampling trains were incorporated. In addition temperature, relative humidity and CO<sub>2</sub> concentration were measured by Indoor Air Quality Monitor PS32 (Sensotron, Poland).

Figure 2: Experimental set up of the instruments.

### 2.3 Estimation of air exchange rate

Measurements of CO<sub>2</sub> concentration revealed periodical increase and decrease of CO<sub>2</sub> levels indoors. The concentrations started to grow daily at the beginning of the visiting hours, reached maximum at the end of the visiting hours and followed by a gradual decrease to the original values. The increase resulted from carbon dioxide exhaled by visitors [24] and the decrease from air exchange between indoors and outdoors.

Hence, the air exchange rate of the library was estimated from the decay in CO<sub>2</sub> concentration during night-time. CO<sub>2</sub> concentration followed an exponential decay with time by [44]:

$$a = \frac{1}{(t - t_o)} \ln \left( \frac{C - C_{out}}{C_o - C_{out}} \right) \quad (1)$$

where,  $a$  is the air exchange rate ( $\text{h}^{-1}$ ),  $t$  and  $t_o$  are the end and beginning of the decay curve ( $\text{h}^{-1}$ ), respectively,  $C$  and  $C_o$  are the CO<sub>2</sub> concentrations (ppm) measured at times  $t$  and  $t_o$ , respectively and

$C_{out}$  (ppm) is the outdoor concentration at time  $t$ . The air exchange rates, estimated for all three campaigns are given in Table 1.

Seasonal variation in air exchange rate indicates different ventilation of the library through the building envelope for different seasons. In naturally ventilated buildings, the airflow is driven by temperature or pressure differences [45]. It is likely that the variation of the ventilation inside the Baroque Library Hall is driven by temperature differences [22]. Table 1 provides the average indoor/outdoor temperature during visiting and non-visiting hours. The numbers strongly suggest that the temperature inside the library depends on outdoor conditions.

Table 1: a) Estimated air exchange rates for each sampling period and b) average ( $\pm$  SD) temperature inside and outside the library for visiting and non-visiting hours for the three seasons.

a)		Spring	Summer	Winter
Air exchange rate ( $\text{h}^{-1}$ )		0.13	0.11	0.15
b)		Temperature		
Indoor	Visiting hours	13.4 ( $\pm$ 0.6)	24.1 ( $\pm$ 0.3)	13.2 ( $\pm$ 1.6)
	Non-visiting hours	13.0 ( $\pm$ 0.5)	24.0 ( $\pm$ 0.3)	13.3 ( $\pm$ 0.5)
Outdoor	Visiting hours	8.4 ( $\pm$ 1.7)	23.9 ( $\pm$ 4.6)	9.2 ( $\pm$ 3.1)
	Non-visiting hours	6.7 ( $\pm$ 1.6)	19.5 ( $\pm$ 3.7)	8.2 ( $\pm$ 2.8)

## 2.4 Indoor mass balance model

The indoor particle concentration for a well-mixed air volume can be described using a dynamic mass balance model:

$$\frac{dC_{in}}{dt} = PaC_{out} - aC_{in} - kC_{in} + \frac{S}{V} \quad (2)$$

where,  $C_{in}$  is the indoor particle concentration ( $\text{cm}^{-3}$ ),  $C_{out}$  is the outdoor particle concentration ( $\text{cm}^{-3}$ ),  $P$  is the penetration efficiency,  $a$  is the air exchange rate ( $\text{h}^{-1}$ ),  $k$  is the deposition rate ( $\text{h}^{-1}$ ),  $S$  is the emission rate of particles ( $\text{h}^{-1}$ ),  $V$  is volume of the area under study ( $\text{cm}^{-3}$ ), and  $t$  is the time (h). The equation (2) assumes that the indoor particle concentration is a result of particle penetration from outdoors, deposition on indoor surfaces, air exchange from indoors to outdoors and emissions from indoor sources. Condensation and coagulation of indoor particles are considered negligible. The assumption of the well-mixed volume was confirmed by examining the spatial variability of the indoor air inside the library. The results indicated that the well-mixed assumption was reasonable.

Indoor particle concentration can be determined using equation (2) for a given time period. For each time step of the specified period, the indoor concentration is estimated using a numerical backward difference:

$$C_{in}(t) = PaC_{out}(t-1)dt + [1 - (a + k)dt]C_{in}(t-1) + \frac{S}{V}dt \quad (3)$$

Under the condition where no sources are present indoors the last term of the above equation can be neglected, and equation (3) is transformed into:

$$C_{in}(t) = PaC_{out}(t-1)dt + [1 - (a + k)dt]C_{in}(t-1) \quad (4)$$

Hence, equation (4) can be used to estimate indoor concentration by selecting the appropriate values for deposition and penetration, when the air exchange rate and the outdoor concentration are known. Both variables ( $k$  and  $P$ ) depend substantially on particle size and characteristics of the building envelope.

Moreover, considering steady state conditions inside the building and no presence of indoor sources equation (2) yields the infiltration factor:

$$F_{inf} = \frac{C_{in}}{C_{out}} = \frac{aP}{a + k} \quad (5)$$

The infiltration factor,  $F_{inf}$ , is a function of air exchange rate  $a$ , penetration efficiency  $P$ , and deposition rate  $k$ . Therefore,  $F_{inf}$  is dimensionless and represents the fraction of particles that penetrate from outdoors and remains suspended indoors. The equation (5) also demonstrates that the infiltration factor is equivalent with the I/O ratio under steady state conditions.

### 3. Results and discussion

#### 3.1 Indoor and outdoor particle characteristics

The total average particle number concentration (both indoors and outdoors) for the three seasons is presented in Table 2. Additionally, Table 2 compares the particle number concentration at different size fractions. The SMPS data were separated into two size fractions, where, the first one includes the particles between 0.014-0.1  $\mu\text{m}$  (nucleation fraction) and the second one includes particles between 0.10-0.71  $\mu\text{m}$  (accumulation fraction). On the other hand, the APS data were separated to the fine

fraction corresponding to particles in the size range of 0.7-3  $\mu\text{m}$  and to the coarse fraction corresponding to particles at the size range of 3-20  $\mu\text{m}$ .

Table 2: Indoor and outdoor particle number concentration ( $\text{cm}^{-3}$ ) for the three seasons. Comparison between the average ( $\pm\text{SD}$ ) total concentration and the average ( $\pm\text{SD}$ ) concentration at different size fractions.

	Total (0.014-0.71 $\mu\text{m}$ )	0.014-0.1 $\mu\text{m}$	0.10-0.71 $\mu\text{m}$	Total (0.7-20 $\mu\text{m}$ )	0.7-3 $\mu\text{m}$	3-20 $\mu\text{m}$
<i>a) Spring</i>						
Indoor	2,301 $\pm$ 742	1,616 $\pm$ 526	686 $\pm$ 253	9.2 $\pm$ 6.2	3.5 $\pm$ 2.2	0.005 $\pm$ 0.004
Outdoor	5,130 $\pm$ 2,751	3,950 $\pm$ 2,152	1,180 $\pm$ 774	29.5 $\pm$ 26.8	12.4 $\pm$ 10.2	0.07 $\pm$ 0.06
<i>b) Summer</i>						
Indoor	2,382 $\pm$ 836	1,565 $\pm$ 549	817 $\pm$ 333	1.7 $\pm$ 0.6	0.8 $\pm$ 0.2	0.01 $\pm$ 0.009
Outdoor	6,379 $\pm$ 4,232	5,079 $\pm$ 3,444	1,299 $\pm$ 940	4.5 $\pm$ 2.9	2.2 $\pm$ 1.2	0.07 $\pm$ 0.05
<i>c) Winter</i>						
Indoor	2,608 $\pm$ 1,201	1,653 $\pm$ 713	955 $\pm$ 534	11.6 $\pm$ 10.0	4.0 $\pm$ 3.1	0.009 $\pm$ 0.008
Outdoor	5,489 $\pm$ 3,414	3,948 $\pm$ 2,431	1,541 $\pm$ 1,122	27.0 $\pm$ 28.1	10.1 $\pm$ 9.3	0.08 $\pm$ 0.06

Higher outdoor concentration observed in all three seasons. The average indoor concentration in the particle size 0.014 - 0.71  $\mu\text{m}$  varied between 2,301 - 2,608  $\text{cm}^{-3}$  during the three seasons, whereas, the average outdoor concentration for the same particle size ranged between 5,130 - 6,379  $\text{cm}^{-3}$ . The numbers indicate higher outdoor concentration by 2-3 orders of magnitude than the indoor number concentration. The same characteristic was observed for bigger particles (0.7-20  $\mu\text{m}$ ).

Table 2 also suggests that particles at lower size fractions (0.014-0.1  $\mu\text{m}$ , 0.7-3  $\mu\text{m}$ ) present higher ambient concentration both indoors and outdoors, than particles at higher fractions (0.10-0.71  $\mu\text{m}$ , 3-20  $\mu\text{m}$ ). Additionally, particle number concentration for sizes  $>$  3  $\mu\text{m}$  was negligible both indoors and outdoors. Similar characteristic was found in [9] in a study at Plantin-Moretus museum in Antwerp, Belgium.

Moreover, it was found that during several periods the indoor particle concentration is highly affected by the outdoor one. Figure 3 presents such a period, where, the indoor and outdoor particle concentrations are plotted during a 4-days period in winter season. It is demonstrated that the temporal fluctuations of outdoor concentration contribute significantly to the indoor ones resulting in a considerable increase of indoor particle concentration for both low (0.014-0.71  $\mu\text{m}$ ) and high (0.7-20  $\mu\text{m}$ ) particle sizes. Similar periods, where the temporal fluctuations of outdoor concentration affected the indoor concentration found in all three seasons, underlying that the particulate matter inside the

library is strongly affected by outdoor conditions. Indoor-outdoor relationship of ambient PM is reported in other studies dealing with museum environments [7,18,21,25,46].

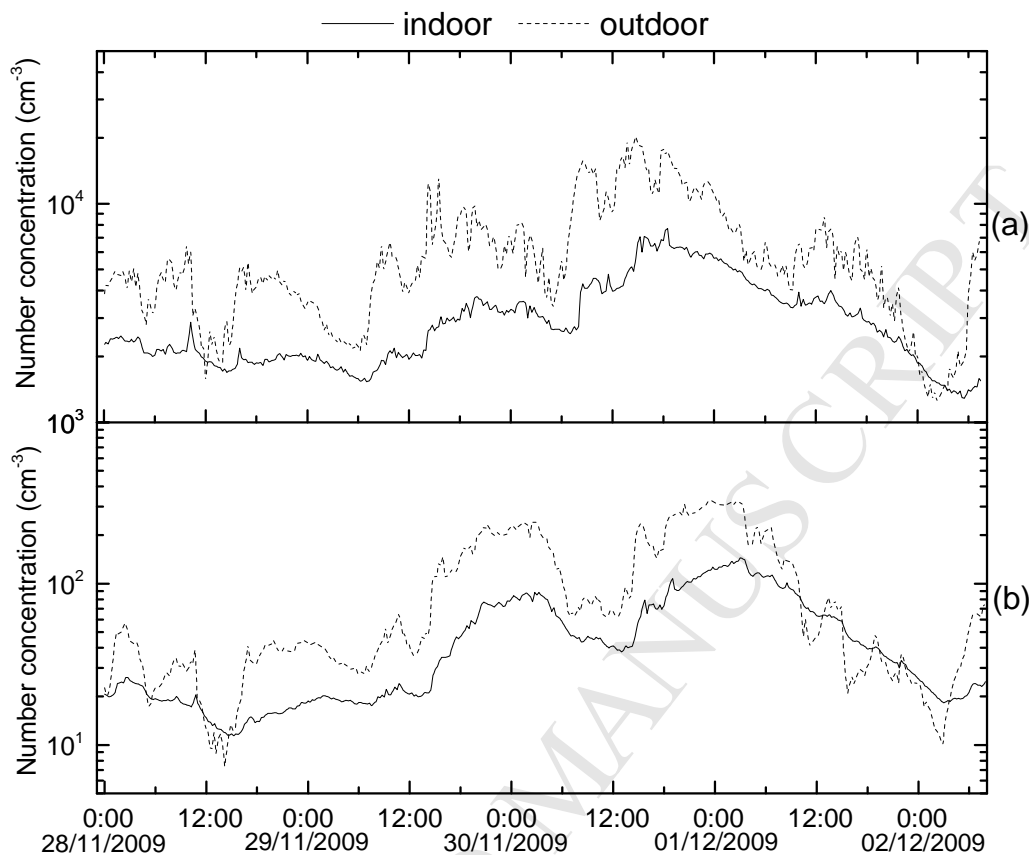


Figure 3: Total indoor and outdoor number concentration of particles in the size range: a) 0.014 - 0.71  $\mu\text{m}$  and b) 0.7 - 20  $\mu\text{m}$  during 28/11/2009-02/12/2009 in winter period.

### 3.2 Indoor/Outdoor Ratio

In general, I/O ratio maintained values lower than 0.7, indicating that there was no significant indoor source (Figure 4). Although, Figure 3 suggests that the indoor concentration is considerably influenced by the outdoor, the relatively low I/O ratio ( $< 0.7$ ) underlay that the building envelope obstructs a significant fraction of outdoor particles penetrate indoors.

Figure 4 also indicates that the I/O ratio depends strongly on particle size. Higher ratios (0.4-0.7) observed in the accumulation fraction (0.1-0.7  $\mu\text{m}$ ) for all three seasons suggest that particle infiltration is more effective at this size range. Lower ratios obtained mainly for ultrafine (0.014-0.1  $\mu\text{m}$ ) and coarse (1-20  $\mu\text{m}$ ) particles. Diffusion due to Brownian motion for ultrafine particles and gravitational settling for coarse particles can explain the lower ratios at these size fractions [47]. Similar dependence of I/O ratio with particle size is reported in other studies [35,39,48]. Additionally, averaged higher ratio of ultrafine particles (0.38) compared to coarse particles (0.27) suggests that

particles at the size range of 0.014-0.1  $\mu\text{m}$  penetrate easier through cracks and leaks inside the library. On the other hand, coarse particles are more effectively removed due to their size [10].

No seasonal variation of I/O ratio observed, since Figure 4 indicates similar ratios through the different seasons. However, it is worth to note the decreased I/O ratio for ultrafine particles (0.014-0.1  $\mu\text{m}$ ) during summer and increased for coarse particles (1-20  $\mu\text{m}$ ) in respect to spring and winter season. It is possible that ultrafine particles present slightly higher values during spring and winter due to higher exchange rate, whereas, the effect from the presence of people in summer season contributes to higher I/O ratios for coarse particles in this season.

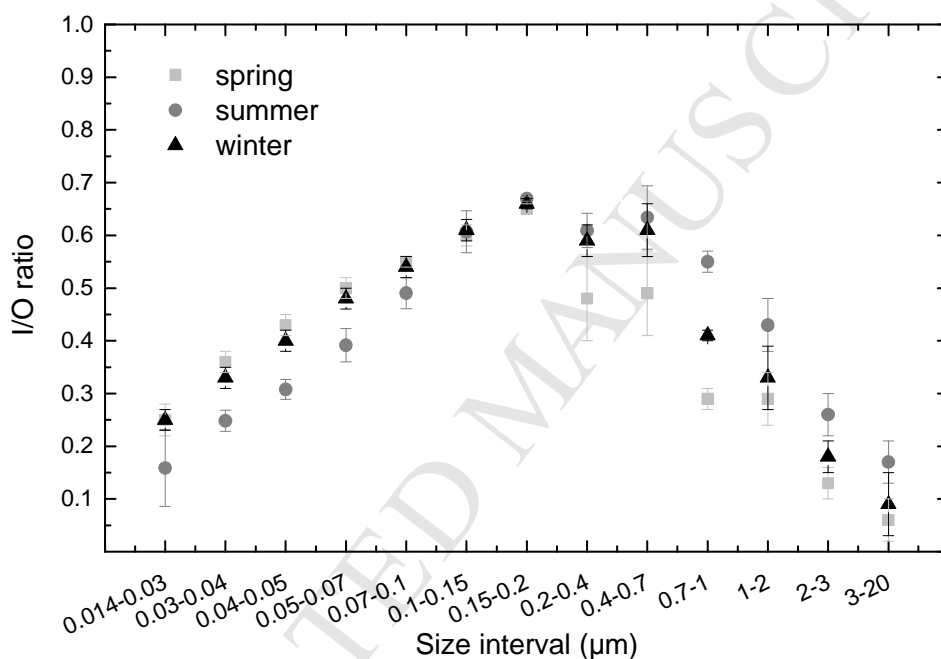


Figure 4: Averaged I/O ratio versus particle size for the three seasons. Error bars represent standard deviation.

### 3.3 Modeling of the indoor particle concentration

#### 3.3.1 Method for estimating deposition rate and penetration efficiency

Indoor particle concentration was modeled for different size intervals using equation (4). Since, the air exchange rate of the library was estimated by  $\text{CO}_2$  measurements, the only requirements in equation (4) is to find the appropriate values for deposition rate  $k$  and penetration efficiency  $P$  using the continuous outdoor particle concentration.

Particle number concentration in the range 0.014-0.7  $\mu\text{m}$  was evaluated using 9 size intervals, whereas, particle number concentration between 0.7-20  $\mu\text{m}$  was evaluated using 4 size intervals. Particle size distribution above 3  $\mu\text{m}$  was not divided into smaller size intervals because indoor

number concentration above  $5 \mu\text{m}$  was usually close to zero. In total 13 discrete size intervals were used to cover the full size range of the measured size distribution. The deposition rate and penetration efficiency were evaluated in each size interval for all three seasons, thus, 3 possible values for each variable in order to obtain an independent result. Valid values for  $P$  were considered inside the range  $0 < P < 1$ , whereas,  $k$  was evaluated for positive values. In order to diminish the possible acceptable values for deposition, a lower limit was used based on the air exchange rate of each season. The lower limit was obtained considering an initial value, which, corresponds to the lowest positive number of the same order of magnitude for each air exchange rate (e.g. for air exchange rate  $0.0022 \text{ min}^{-1}$  the initial value was selected at  $0.0001 \text{ min}^{-1}$ ). The above method was used in equation (4) in order to ensure that the deposition rate retains mathematically significant value. The time step used in equation (4) was selected the same with the time interval used in the measurement, thus, 5 minutes. Hence, the deposition rate was originally obtained in units  $\text{min}^{-1}$  and the modeled values were exactly same in number as the measured data. The modeled was running each time for a selected value of  $k$  and for the full range of  $P$ . The time step for penetration was chosen 0.01, whereas, for deposition  $0.0005 \text{ min}^{-1}$  (or  $0.03 \text{ hr}^{-1}$ ).

The aim was to find the best fit between the measured indoor concentration and the obtained modeled indoor concentration. This was succeeded by finding the pair of values ( $k$ ,  $P$ ) that generate the best fitted curve. For this purpose, coefficient of determination ( $R^2$ ) was used as a criterion. Nevertheless, in many cases more than one pair of  $k$  and  $P$  resulted in nearly equal values of  $R^2$ . The same problem is reported in similar studies dealing with infiltration in houses [39,40]. The methodology followed to overcome this problem was to find one pair that generates a curve with the highest  $R^2$  value. Then, the highest value of  $R^2$  was selected, and only the  $R^2$  values higher than the 95% of the best generated  $R^2$  were considered valid. Any pair of  $k$  and  $P$  corresponding to a valid  $R^2$  was selected to determine the averaged  $k$  and  $P$  for each size interval. Thus, the final deposition and penetration was obtained from several valid pairs of  $k$  and  $P$ . Table 3 lists the deposition rate  $k$  and penetration efficiency  $P$  in each size interval for the 3 seasons.

The above method resulted in one unique value of  $R^2$  with highest correlation for every tested deposition rate in the range of the penetration efficiency (0.01-0.99). Plotting every one of these  $R^2$  values with deposition, we obtain a U-shaped curve similar to the one Bennett and Koutrakis [39] found (Figure 5a). The U-shaped curve suggests that there was always one  $R^2$  value, which gave the best correlation between the measured and the modeled concentration but also indicates the presence of other almost equal values. Thus, highlights the non-unique solution of  $k$  and  $P$  and reflects the variability of the results with all possibly acceptable values. Furthermore, using the  $P$  value that corresponds to the previously found  $R^2$  we obtain a proportional relationship between  $k$  and  $P$ . Figure 5b plots the  $k$  and  $P$  pairs for two selected size intervals ( $0.014 - 0.03 \mu\text{m}$ ,  $0.03 - 0.04 \mu\text{m}$ ) for the three

seasons. The values of  $P$  in each case represent the best correlation ( $R^2$ ) for each deposition rate in each size interval. It is demonstrated that  $k$  and  $P$  not only depend proportionally but are characterized by a linear relationship. The same characteristic found in all cases for all three seasons. Hence, it is highlighted that the two model parameters are not independent, rather than, when deposition increases (higher settling) model formulation requires an increased penetration efficiency (higher fraction of outdoor particles penetrate indoors) in order to find the best fit between the measured and the modeled concentration.

Moreover, in order to avoid the influence of the starting point, any local maximum of the indoor concentration at the beginning of the dataset was neglected. Such a local maximum was found at the beginning of winter, where, the data from the first 20 hours were excluded from the calculations. Additionally, in summer season it was generally observed that the modeled values presented a significant underestimation of indoor concentration only at the end of the dataset. Hence, it was concluded that the starting point (which presented remarkably high indoor concentration compared to the rest of the data) influences the results and the data were modeled at different starting points. No underestimation of indoor concentration was obtained when the starting point was located at the middle of the data set (18/07/2009). All subsequent calculations were computed using the previously found starting point.

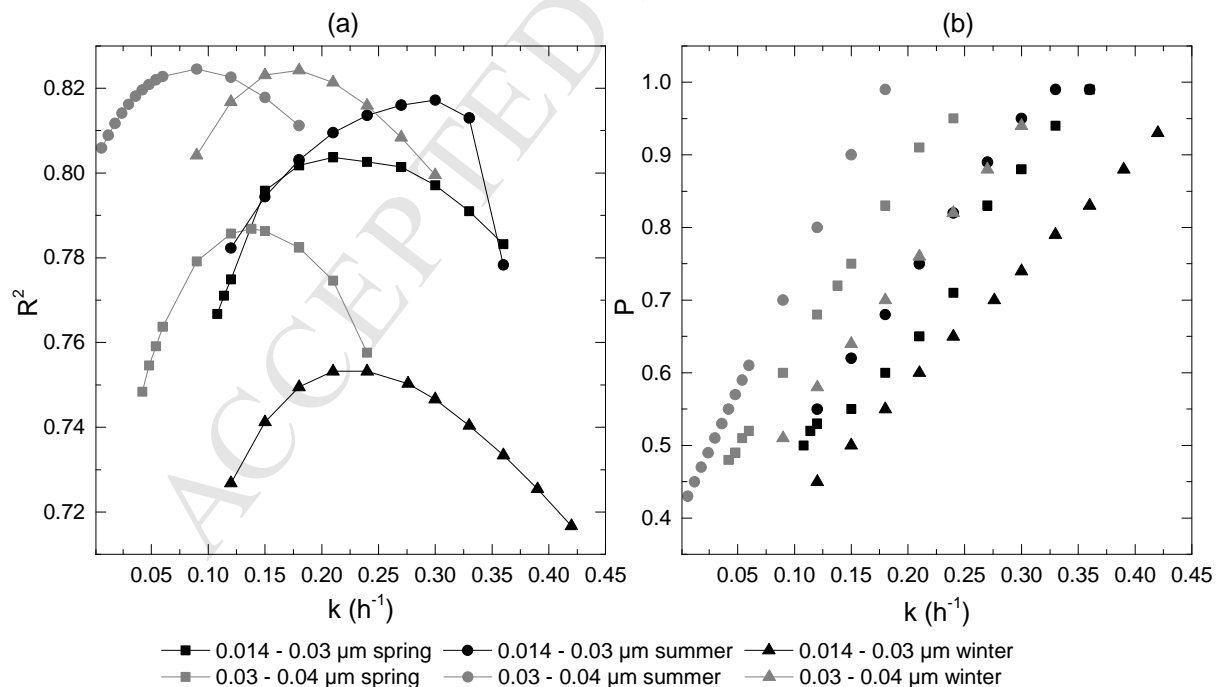


Figure 5: a) Highest generated  $R^2$  for each deposition rate at two selected size intervals (0.014 - 0.03  $\mu m$ , 0.03 - 0.04  $\mu m$ ), b) Penetration efficiency (that corresponds to highest  $R^2$ ) versus deposition rate for the same selected size intervals.

Measured data and modeled concentration were in general in good agreement. High  $R^2$  values were usually found ( $> 0.7$ ) with good correlation between the compared values. Figure 6 provides, as an example, a comparison between the measured indoor concentration and the modelled one for two size intervals in each season. It can be seen that a simple mass balance model accounting particle infiltration, exchange rate with the outdoor environment and deposition losses is suitable enough to reproduce the observed concentration. High correlation ( $R^2$ ) suggests good agreement between the measured data and the modelled values.

In some cases, however, the model could not achieve high levels of confidence, although, the generated curve was similar to the profile of the indoor concentration. The low  $R^2$  was mainly due to strong fluctuations of indoor and outdoor concentration and was observed mainly during summer season. However, the estimated  $k$  and  $P$  were not excluded in order to compare it with averaged I/O ratio.

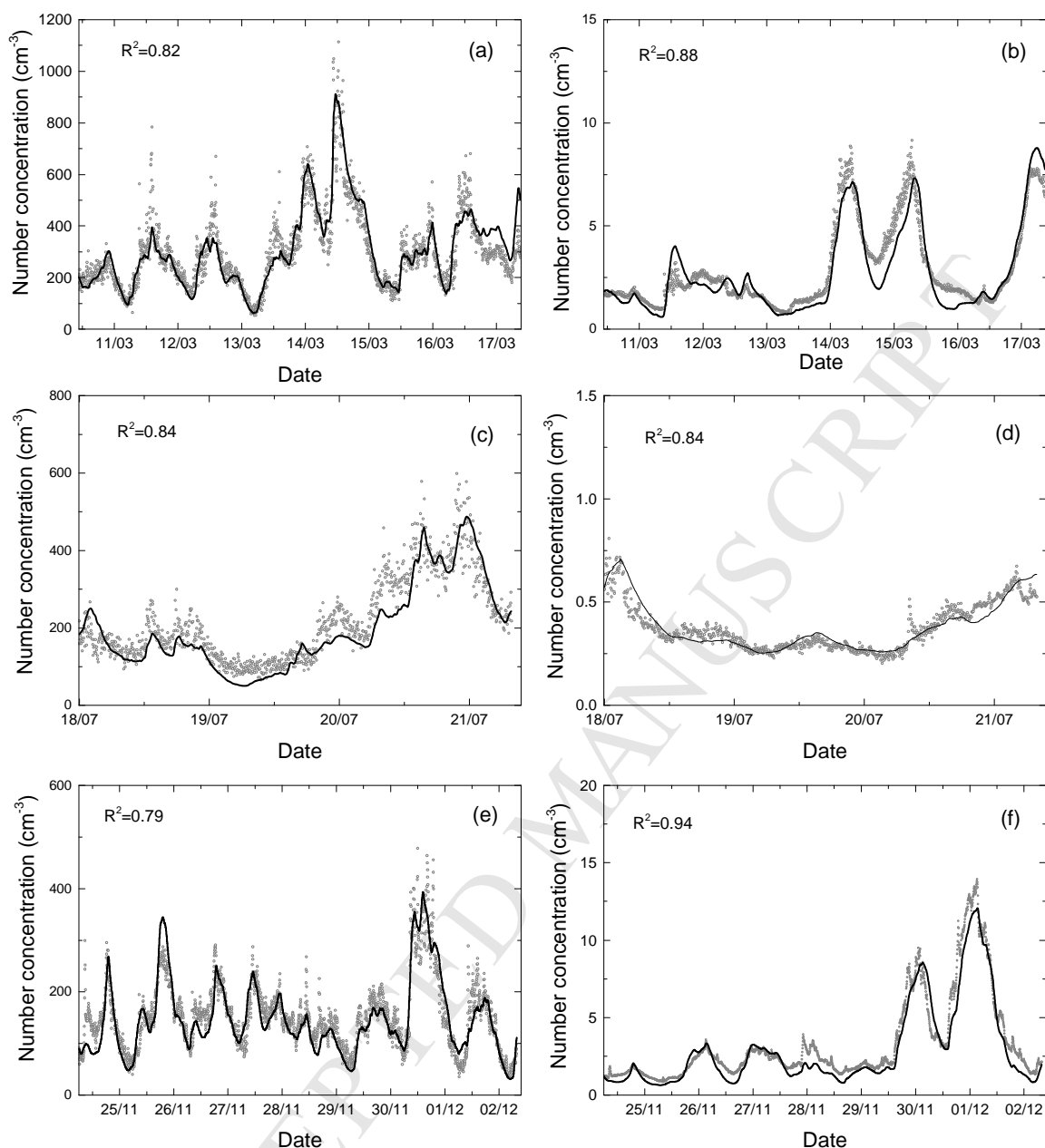


Figure 6: Comparison between measured indoor concentration (○) and modeled indoor concentration (—) using the best fitted values of  $k$  and  $P$  for two size intervals (0.014-0.1  $\mu\text{m}$ , 0.7-1  $\mu\text{m}$ ) and all three season. Plots a, c and e correspond to particles at the size range 0.014-0.1  $\mu\text{m}$  for spring, summer and winter respectively. Plots b, d and f correspond to particles at the size range 0.7-1  $\mu\text{m}$  for spring, summer and winter respectively. The pairs of  $k$  and  $P$  are taken from Table 3. The correlation ( $R^2$ ) between the measured data and modeled values is also presented.

Finally, in the size interval 3-20  $\mu\text{m}$  the correlation between the measured data and the modeled values was substantially lower than the other tested size intervals. It was found that the model failed to generate several peaks of indoor particle concentration. Although, the indoor concentration of coarse particles at the size interval 3-20  $\mu\text{m}$  was negligible in all three seasons, it was assumed that this

fraction of particles is mostly affected by the presence of visitors inside the library. Other studies dealing with air pollution in museums reported the influence of visitors on the indoor concentration at coarse particle fraction [7-9,26,49]. Thus, in order to determine appropriate values of  $k$  and  $P$  for coarse particles, the indoor concentration was compared in parallel with the outdoor. We then isolated time periods, where, the indoor concentration followed similar temporal fluctuations as the outdoor and investigated only these selected periods to obtain values for deposition and penetration. Originally, only the night data of each season were examined but no good correlation was found because the evaluation of only the night data resulted in shorter tested periods, which were not representative enough.

Table 3: Estimated values of deposition and penetration using equation (4) and area-averaged deposition velocity,  $\bar{V}_d$ . The values represent the average and standard deviation (mean  $\pm$  SD) of  $k$  and  $P$  in each size interval.

Size interval ( $\mu\text{m}$ )	$k$ ( $\text{h}^{-1}$ )	$P$	$\bar{V}_d$ (m/s) ( $\cdot 10^{-5}$ )
Spring			
0.014 - 0.03	$0.22 \pm 0.09$	$0.75 \pm 0.15$	6.04
0.03 - 0.04	$0.12 \pm 0.07$	$0.74 \pm 0.15$	3.29
0.04 - 0.05	$0.05 \pm 0.04$	$0.69 \pm 0.15$	1.37
0.05 - 0.07	$0.03 \pm 0.02$	$0.63 \pm 0.08$	0.82
0.07 - 0.1	$0.03 \pm 0.02$	$0.68 \pm 0.08$	0.82
0.1 - 0.15	$0.02 \pm 0.01$	$0.68 \pm 0.06$	0.55
0.15 - 0.2	$0.02 \pm 0.01$	$0.72 \pm 0.05$	0.55
0.2 - 0.4	$0.03 \pm 0.02$	$0.65 \pm 0.07$	0.82
0.4 - 0.7	$0.03 \pm 0.02$	$0.58 \pm 0.08$	0.82
0.7 - 1	$0.15 \pm 0.10$	$0.60 \pm 0.17$	4.12
1 - 2	$0.11 \pm 0.07$	$0.54 \pm 0.14$	3.02
2 - 3	$0.35 \pm 0.15$	$0.51 \pm 0.15$	9.61
3 - 20	$1.04 \pm 0.39$	$0.46 \pm 0.13$	28.58
Summer			
0.014 - 0.03	$0.24 \pm 0.08$	$0.77 \pm 0.13$	6.60
0.03 - 0.04	$0.06 \pm 0.05$	$0.70 \pm 0.17$	1.65
0.04 - 0.05	$0.04 \pm 0.02$	$0.65 \pm 0.11$	1.10
0.05 - 0.07	$0.03 \pm 0.02$	$0.70 \pm 0.09$	0.82
0.07 - 0.1	$0.03 \pm 0.02$	$0.82 \pm 0.09$	0.82
0.1 - 0.15	$0.009 \pm 0.004$	$0.80 \pm 0.03$	0.02
0.15 - 0.2	$0.009 \pm 0.004$	$0.83 \pm 0.02$	0.02
0.2 - 0.4	0.006*	$0.76 \pm 0.02$	0.02
0.4 - 0.7	0.006*	$0.76 \pm 0.03$	0.02
0.7 - 1	$0.03 \pm 0.01$	$0.69 \pm 0.07$	0.82
1 - 2	$0.06 \pm 0.05$	$0.76 \pm 0.15$	1.65
2 - 3	$0.08 \pm 0.04$	$0.48 \pm 0.07$	2.20
3 - 20	$0.70 \pm 0.07$	$0.70 \pm 0.06$	19.24
Winter			
0.014 - 0.03	$0.27 \pm 0.10$	$0.69 \pm 0.15$	7.42
0.03 - 0.04	$0.20 \pm 0.07$	$0.74 \pm 0.15$	5.50

0.04 - 0.05	0.11 ± 0.07	0.73 ± 0.15	3.02
0.05 - 0.07	0.05 ± 0.04	0.72 ± 0.15	1.37
0.07 - 0.1	0.05 ± 0.03	0.75 ± 0.14	1.37
0.1 - 0.15	0.04 ± 0.02	0.77 ± 0.13	1.10
0.15 - 0.2	0.04 ± 0.02	0.79 ± 0.11	1.10
0.2 - 0.4	0.04 ± 0.02	0.77 ± 0.13	1.10
0.4 - 0.7	0.04 ± 0.02	0.74 ± 0.13	1.10
0.7 - 1	0.15 ± 0.08	0.73 ± 0.16	4.12
1 - 2	0.17 ± 0.09	0.71 ± 0.17	4.67
2 - 3	0.41 ± 0.17	0.67 ± 0.19	11.27
3 - 20	1.09 ± 0.27	0.76 ± 0.14	29.95

\* no standard deviation. Deposition determined only from one value of k.

### 3.3.2 Averaged values of $k$ and $P$

The deposition rate varied substantially with particle size. The highest rates were obtained for particle size 3-20  $\mu\text{m}$  (1.04, 0.70 and 1.09  $\text{h}^{-1}$  for spring, summer and winter respectively). Higher particle size is associated with higher deposition rates due to strong gravitational settling that characterizes coarse particles. A similar trend but with lower rates was observed for ultrafine particles. High deposition rates (0.22-0.27  $\text{h}^{-1}$ ) were obtained for nucleation fraction 0.014-0.03  $\mu\text{m}$  in all three seasons caused mainly by Brownian diffusion. On the other hand, deposition for particles at accumulation fraction (0.1-0.7  $\mu\text{m}$ ) preserved nearly the same values (0.02-0.03  $\text{h}^{-1}$  in spring, 0.006-0.009  $\text{h}^{-1}$  in summer and 0.04  $\text{h}^{-1}$  in winter). The above findings are in agreement with other studies [13,14,34,35,39,40,44,50,51] where deposition was found to depend considerably on particle size. The values also indicate nearly similar rates for the three seasons.

Although, deposition was found to depend on particle size, penetration efficiency, on the other hand, was not clearly related with particle size. High penetration (0.6 - 0.8) was found in most size intervals. The numbers suggest that outdoor particles penetrate easily inside the library independent of the particle size. High penetration (0.8-0.9) in ultrafine particles is also reported in literature [16,35], but coarse particles are usually characterized with lower penetration factors due to their size, which, prevents them from entering the building [52]. Although, such a trend is observed in spring season, penetration during summer (0.70) and winter (0.76) seasons retained high estimates at coarse particles. Higher estimates of penetration efficiency than expected (in particle sizes  $> 1 \mu\text{m}$ ) are reported in [13,53]. It is likely that high penetration is due to the building envelope. Experiments conducted in laboratories associated the increased values with higher pressure difference or larger crack height [16]. Additionally, geometry of the cracks has been found to considerably affect penetration factors [54]. A possible reason since the library corresponds to an old construction.

Figure 7 presents a comparison of the averaged  $k$  and  $P$  in the present study with values from the literature corresponding in real environments. In general, our estimates are comparable with literature

values. However, it is observed that deposition for accumulation fraction (0.1-0.7  $\mu\text{m}$ ) presents the lowest rates than literature values. Different characteristics of the indoor environments (volume, air flow turbulence, surface texture roughness, mixing mechanisms) influence the results considerably [55]. An easy way to interpret and compare the results is to introduce the area-averaged deposition velocity (Table 3). Using the relation  $\bar{V}_d = k(V / \Sigma S)$  [55], where  $\bar{V}_d$  is the area-averaged deposition velocity,  $V$  represents the volume of the library ( $\text{m}^3$ ) and  $S$  the surface area ( $\text{m}^2$ ). The surface area was determined including all books and shelves and surface to volume ratio was found at  $1.01 \text{ m}^{-1}$ . Thus, the deposition rate  $k$  was transformed into the area-averaged deposition velocity  $\bar{V}_d$ . Likewise higher velocities were obtained for ultrafine and coarse particles. Table 3 suggests that deposition velocity inside the library ranged between  $10^{-6}$ - $10^{-4}$  m/s, which is in full agreement with literature values ( $10^{-6}$ - $10^{-3}$  m/s [55]).

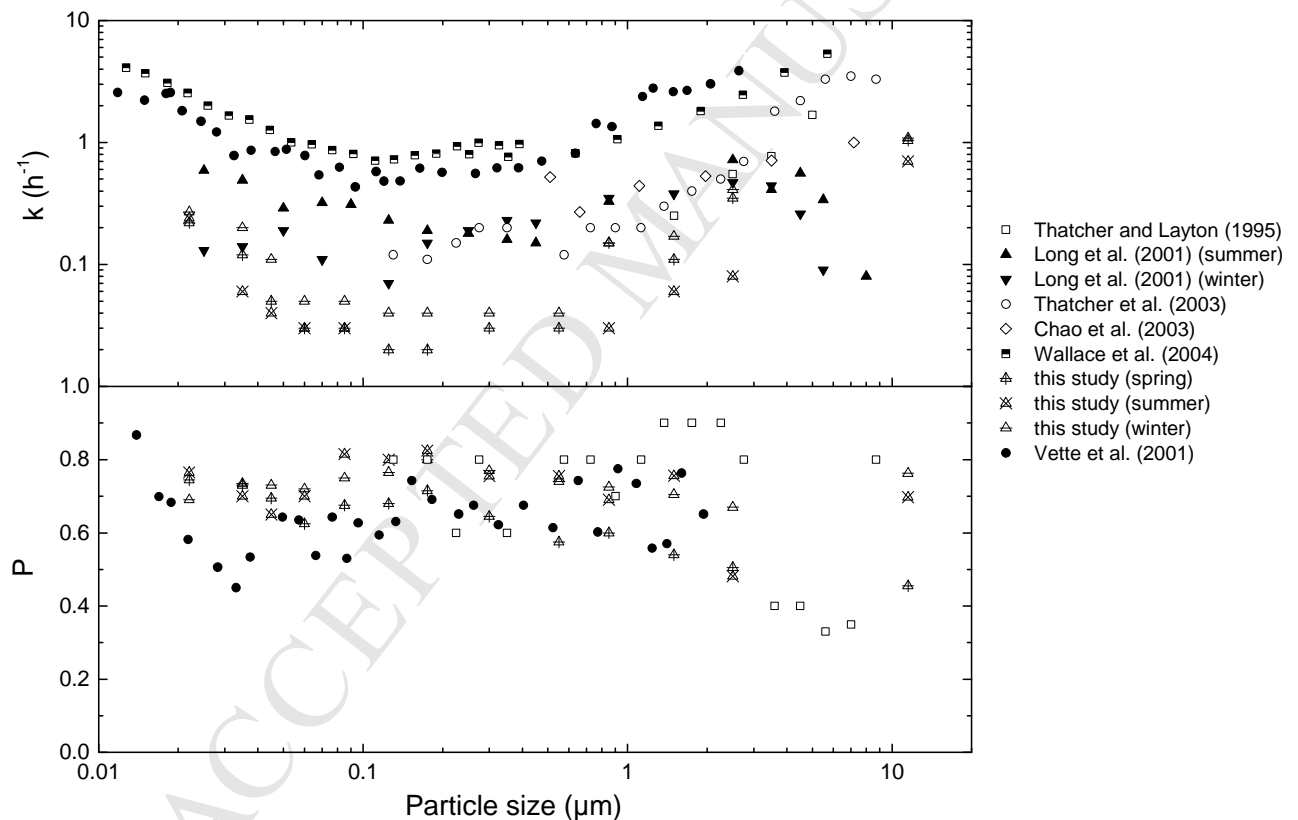


Figure 7: Comparison between averaged deposition rate and penetration efficiency in this study with studies from literature [13,35,36,53,56,57] in real environments.

### 3.4 Infiltration factor and comparison with I/O ratio

The infiltration factor for each size interval was calculated using deposition and penetration values provided in Table 3 and the corresponding air exchange rate for each season (Table 1). Evaluation of

the estimated  $k$  and  $P$  was achieved comparing infiltration factor with I/O ratio. Figure 8 compares the infiltration factor with I/O ratio at each size interval for the three seasons. It should be noted that in the case of coarse fraction (3-20  $\mu\text{m}$ ) the I/O ratio presented in Figure 8 corresponds to the calculated I/O ratio from the number concentration data of the selected periods, used to determine  $k$  and  $P$  at this size range.

Infiltration factor was equal to I/O ratio in most cases. Figure 9 plots the infiltration factor versus I/O ratio for all size intervals and seasons. Good agreement with I/O ratio ensures that the averaged  $k$  and  $P$  represent at a high confidence level the particle deposition rate and penetration efficiency in each size interval. By extend it also confirms the selection of the starting point in summer data and the selected periods that were used in 3-20  $\mu\text{m}$  size interval to determine  $k$  and  $P$  for coarse particles.

The infiltration factor ranged between 0.24-0.76 for particles in the size range 0.014-0.7  $\mu\text{m}$ , whereas, in the size range 0.7-20  $\mu\text{m}$   $F_{\text{inf}}$  ranged between 0.05-0.56. Since,  $F_{\text{inf}}$  represents the fraction of particles that reaches the indoor environment from outdoors and remains suspended, it indicates that infiltration of ultrafine particles is higher compared to coarse particles and that enrichment of ultrafine particles inside the library was caused by penetration from outdoors. It also confirms that particle dynamics (deposition, penetration) depend on particle size. Similar dependence of  $F_{\text{inf}}$  with particle size was found in other studies [39,40,51].

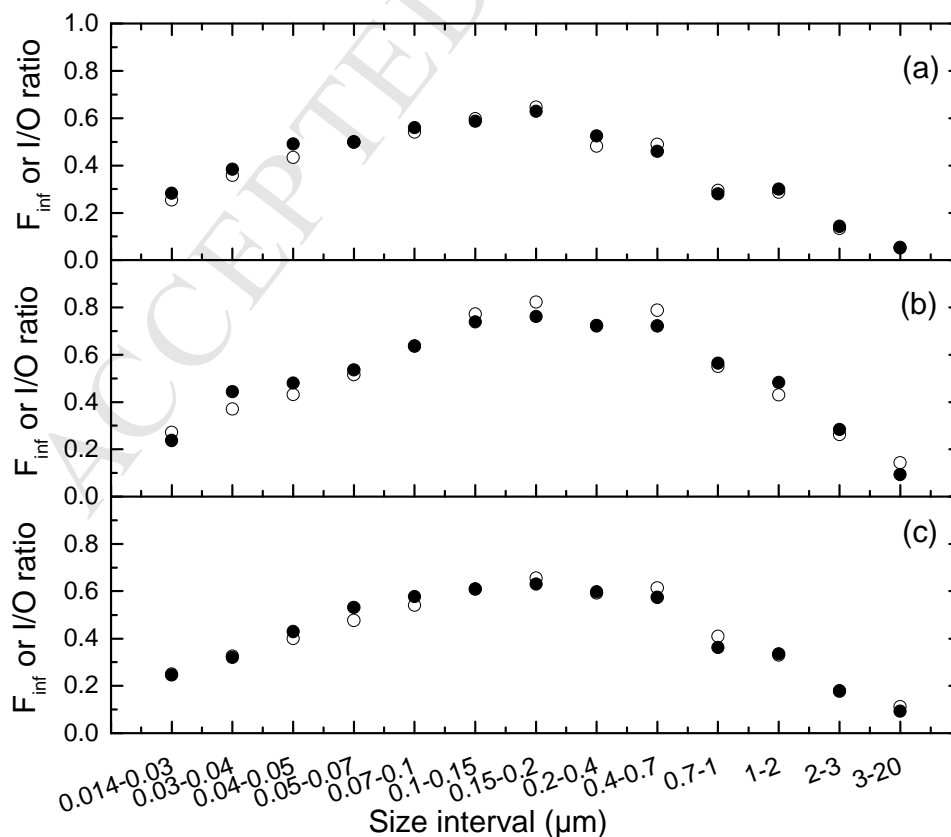


Figure 8: Comparison between infiltration factor (●) and I/O ratio (○) in each size interval for a) spring, b) summer and c) winter seasons.

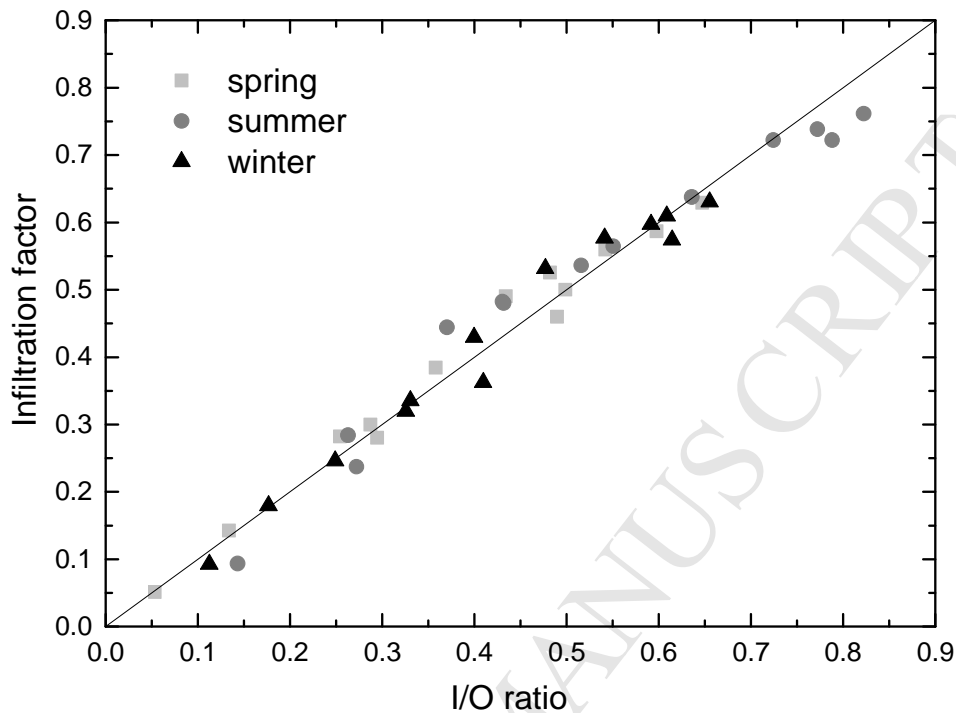


Figure 9: Infiltration factor versus I/O ratio for all size intervals for the three seasons. The line ( $y=x$ ) correlates the two variables.

### 3.5 Influence of visitors inside the library

Periodical increase and decrease of indoor particle concentration that could not be modeled, was found in the size range between 3-20  $\mu\text{m}$  in all three seasons. Figure 10 presents the indoor number concentration of coarse particles for spring season. A comparison with modeled concentration is also shown. Although, modeled concentration successfully represents the indoor concentration at periods outside the visiting hours, there are several temporal indoor fluctuations that the model could not generate. These temporal fluctuations were associated with the presence of visitors inside the library, since all of them were located during visiting hours. Indoor concentration of coarse particles may be elevated for different reasons: transport of dust from outside, resuspension of the deposited particles on the floor, fabric fibers or material emissions. Other studies related the increased indoor concentration at coarse fraction with human presence during the visiting hours [4,9,25,46].

However, a significant deviation of the modeled concentration from the measured data outside the visiting hours was observed at the end of the season (16/07/09 19:00 until the end). This deviation was due to the averaged procedure that was used to derive the averaged values for  $k$  and  $P$ . In particular,

evaluation of the model at this period (16/07/09 19:00 until the end) provided with lower values of P. Thus, modeling the indoor concentration of coarse particles during spring with the averaged P, resulted in higher modeled values than the measured at the end of season. A limitation due to the evaluation of the indoor number concentration of coarse particles in selected time periods.

In order to determine the impact of human presence inside the library, the periods during visiting hours were isolated and compared with periods of non-visiting hours. Table 4 presents the concentration of coarse particles during visiting and non-visiting hours for all three seasons. Indeed, during visiting hours the indoor concentration of coarse particles increased by a factor of 3, 3.2 and 2 for spring, summer and winter respectively, suggesting that human presence influences substantially indoor concentration at this size range (3-20  $\mu\text{m}$ ).

Additionally, Figure 11 presents a comparison of I/O ratios between visiting and non-visiting hours. It is demonstrated that I/O ratios maintain higher values during visiting hours for all three seasons. Moreover, it is observed that higher I/O characterizes summer, which is directly associated with more people visiting the library and longer visiting hours at this season. The 50<sup>th</sup> percentile in summer was 0.24, whereas, for spring and winter season the 50<sup>th</sup> percentile was 0.11 and 0.14 respectively.

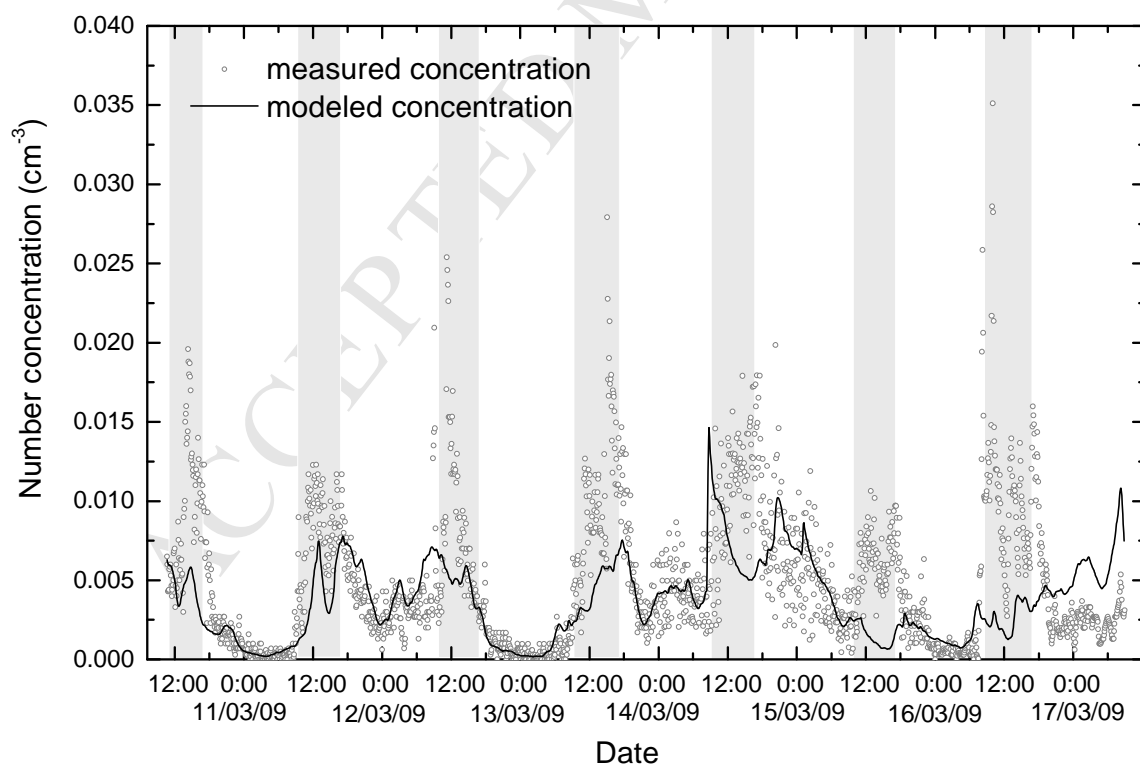


Figure 10: Comparison of indoor measured concentration with modeled concentration of coarse particles (3-20  $\mu\text{m}$ ) in spring season. Colored areas represent visiting hours (10:00-17:00).

Table 4: Averaged number concentration of indoor coarse particles (3-20  $\mu\text{m}$ ) during visiting and non-visiting hours.

	Number concentration ( $\text{cm}^{-3}$ )		
	Visiting hours	Non-visiting hours	Increase factor
Spring (10:00-17:00)	0.009	0.003	3
Summer (10:00-20:00)	0.016	0.005	3.2
Winter (10:00-16:00)	0.014	0.007	2

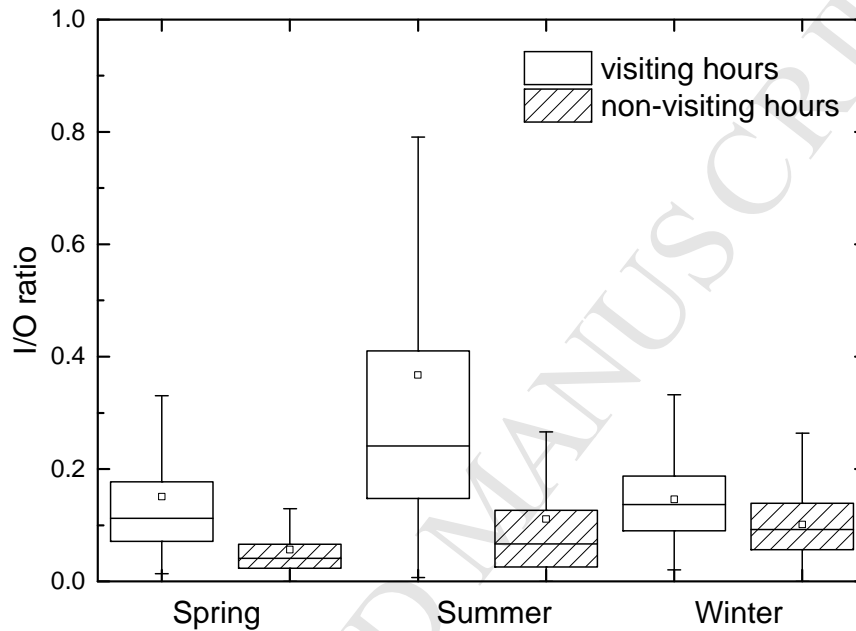


Figure 11: Comparison of I/O ratio of coarse particles (3-20  $\mu\text{m}$ ) for visiting and non-visiting hours. The box plots represent the 25<sup>th</sup> and the 75<sup>th</sup> percentile values, mean value and the horizontal line the median (50<sup>th</sup> percentile) value. Outliers are excluded.

#### 4. Conclusions

Particle number concentration was measured inside a naturally ventilated building during different seasons (spring, summer, winter). It was found that indoor concentration was substantially influenced by outdoor fluctuations in all three periods. No seasonal variation of I/O ratio between the same particle size suggests similar behavior in terms of particle dynamics and building characteristics. A mass balance model was used to evaluate the contribution from outdoors assuming no indoor sources, where the deposition rate and penetration efficiency were evaluated at each size interval for the three seasons.

The present method provided several valid pairs of deposition and penetration at each size interval, suggesting that there is no unique solution and highlighting the variability of  $k$  and  $P$ . Each size interval was examined separately and averaged values of  $k$  and  $P$  were finally used to determine

infiltration factor. The infiltration factor was in good agreement with I/O ratio ensuring the well-estimated values for deposition and penetration at each size interval. It was also evident that the  $F_{inf}$  was size dependent with less effective removal at accumulation fraction. Therefore, indoor concentration was dominated by ultrafine particles, which were associated with penetration from outdoors due to higher infiltration factor. Coarse particles, on the other hand, were associated with human presence due to low confidence level between modeled and measured concentration. In addition, the contribution of the visitors was examined separately, where higher I/O ratio and indoor concentration during visiting hours confirmed the influence from indoor sources.

### Acknowledgement

The experimental work was supported by EEA/Norwegian Financial Mechanisms under grant A/CZ0046/2/001. The modelling work was supported by the European Union 7<sup>th</sup> framework program HEXACOMM FP7/2007-2013 under grant agreement N° 315760.

### References

- [1] Fenger J. Air pollution in the last 50 years - From local to global. *Atmos Environ* 2009;43:13-22.
- [2] Huijbregts Z, Kramer RP, Martens MHJ, van Schijndel AWM, Schellen HL. A proposed method to assess the damage risk of future climate change to museum objects in historic buildings. *Build Environ* 2012;55:43-56.
- [3] Nazaroff WW, Cass GR. Protecting museum collections from soiling due to the deposition of airborne particles. *Atmos Environ* 1991;25:841-52.
- [4] Camuffo D, Brimblecombe P, Van Grieken R, Busse HJ, Sturaro G, Valentino A, et al. Indoor air quality at the Correr Museum, Venice, Italy. *Sci Total Environ* 1999;236:135-52.
- [5] Hatchfield PB. *Pollutants in the museum environment*. London: Archetype Publications; 2005.
- [6] Fenech A, Strlič M, Cigić IK, Levart A, Gibson TL, de Bruin G, et al. Volatile aldehydes in libraries and archives. *Atmos Environ* 2010;44:2067-73.
- [7] Worobiec A, Samek L, Krata A, Van Meel K, Krupinska B, Stefaniak EA, et al. Transport and deposition of airborne pollutants in exhibition areas located in historical buildings-study in Wawel Castle Museum in Cracow, Poland. *J Cult Herit* 2010;11:354-59.

- [8] Godoi RHM, Carneiro BHB, Paralovo SL, Campos VP, Tavares TM, Evangelista H, et al. Indoor air quality of a museum in a subtropical climate: The Oscar Niemeyer museum in Curitiba, Brazil. *Sci Total Environ* 2013;452-453:314-20.
- [9] Krupińska B, Van Grieken R, De Miel K. Air quality monitoring in a museum for preventive conservation: Results of a three-year study in the Plantin-Moretus Museum in Antwerp, Belgium. *Microchem J* 2013;110:350-60.
- [10] Nazaroff WW. Indoor particle dynamics. *Indoor Air* 2004;14:175-83.
- [11] Morawska L, Salthammer T. Indoor environment, Airborne particles and settled dust. Willey-VCH GmbH & Co. KGaA; 2003.
- [12] Glytsos T, Ondráček J, Džumbová L, Kopanakis I, Lazaridis M. Characterization of particulate matter concentrations during controlled indoors activities. *Atmos Environ* 2010;44:1539-49.
- [13] Thatcher TL, Layton DW. Deposition, resuspension, and penetration of particles within a residence. *Atmos Environ* 1995;29:1487-97.
- [14] Liu D-L, Nazaroff WW. Modeling pollutants penetration across building envelopes. *Atmos Environ* 2001;35:4451-62.
- [15] Li Y, Chen Z. A balance-point method for assessing the effect of natural ventilation on indoor particle concentrations. *Atmos Environ* 2003;37:4277-85.
- [16] Chen C, Zhao B. Review of relationship between indoor and outdoor particles: I/O ratio, infiltration factor and penetration factor. *Atmos Environ* 2011;45:275-88.
- [17] Lai ACK, Fung JLS, Li M, Leung KY. Penetration of fine particles through rough cracks. *Atmos Environ* 2012;60:436-43.
- [18] Brimblecombe P, Blades N, Camuffo D, Sturaro G, Valentino A, Gysels K, et al. The indoor environmental of a modern museum building, the Sainsbury Centre for Visual Arts, Norwick, UK. *Indoor Air* 1999;9:146-64.

- [19] Salmon GL, Cass GR, Bruckman K, Haber J. Ozone exposure inside museums in the historic central district of Krakow, Poland. *Atmospheric Environment* 2000;34:3823-32.
- [20] Pavlogeorgatos G. Environmental parameters in museums. *Build Environ* 2003;38:1457-62.
- [21] Gysels K, Delalieux F, Deutsch F, Van Grieken R, Camuffo D, Bernardi A, et al. Indoor environment and conservation in the Royal Museum of Fine Arts, Antwerp, Belgium. *J Cult Herit* 2004;5:221-30.
- [22] López-Aparicio S, Smolík J, Mašková L, Součková M, Grøntoft T, Ondráčková L, et al. Relationship of indoor and outdoor air pollutants in a naturally ventilated historical building envelope. *Build Environ* 2011;46:1460-68.
- [23] Schieweck A, Salthammer T. Indoor air quality in passive-type museum showcases. *J Cult Herit* 2011;12:205-13.
- [24] Varas-Muriel MJ, Fort R, Martínez-Garrido MI, Zorona-Indart A, López-Arce P. Fluctuations in the indoor environment in Spanish rural churches and their effects on heritage conservation: Hydro-thermal and CO<sub>2</sub> conditions monitoring. *Build Environ* 2014;82:92-109.
- [25] Hu T, Lee S, Cao J, Chow JC, Watson JG, Ho K, et al. Characterization of winter airborne particles at Emperor Qin's Terra-cotta Museum, China. *Sci Total Environ* 2009;407:5319-27.
- [26] Ghedini N, Ozga I, Bonazza A, Dilillo M, Cachier H, Sabbioni C. Atmospheric aerosol monitoring as a strategy for the preventive conservation of urban monumental heritage: The Florence Baptistery. *Atmos Environ* 2011;45:5979-87.
- [27] Jones NC, Thornton CA, Mark D, Harrison RM. Indoor/outdoor relationships of particulate matter in domestic homes with roadside, urban and rural locations. *Atmos Environ* 2000;34:2603-12.
- [28] Lunden MM, Thatcher TL, Hering SV, Brown NJ. Use of time- and chemically resolved particulate data to characterize the infiltration of outdoor PM<sub>2.5</sub> into a residence in the San Joaquin Valley. *Environ Sci Technol* 2003;37:4724-32.
- [29] Kopperud RJ, Ferro AR, Hildemann LM. Outdoor versus indoor contributions to indoor particulate matter (PM) determined by mass balance methods. *J Air Waste Manage* 2004;54:1188-96.

- [30] Schneider T, Jensen KA, Clausen PA, Afshari A, Gunnarsen L, Wählén P, et al. Prediction of indoor concentration of 0.5-0.4  $\mu\text{m}$  particles of outdoor origin in an uninhabited apartment. *Atmos Environ* 2004;38:6349-59.
- [31] Polidori A, Arhami M, Sioutas C, Delfino RJ, Allen R. Indoor/outdoor relationships, trends, and carbonaceous content of fine particulate matter in retirement homes of the Los Angeles Basin. *J Air Waste Manage* 2007;57:366-79.
- [32] Lazaridis M, Alexandropoulou V, Hanssen JE, Dye C, Eleftheriadis K, Katsivela E. Inorganic and carbonaceous components in indoor/outdoor particulate matter in two residential houses in Oslo, Norway. *J Air Waste Manage* 2008;58:346-56.
- [33] Tung TCW, Chao CYH, Burnett J. A methodology to investigate the particulate penetration coefficient through building shell. *Atmos Environ* 1999;33:881-93.
- [34] Abt E, Suh HH, Catalano P, Koutrakis P. Relative contribution of outdoor and indoor particle sources to indoor concentrations. *Environ Sci Technol* 2000;34:3579-87.
- [35] Long CM, Suh HH, Catalano PJ, Koutrakis P. Using time- and size- resolved particulate data to quantify indoor penetration and deposition behavior. *Environ Sci Technol* 2001;35:2089-99.
- [36] Thatcher TL, Lunden MM, Revzan KL, Sextro RG, Brown NJ. A concentration rebound method for measuring particle penetration and deposition in the indoor environment. *Aerosol Sci Technol* 2003;37:847-64.
- [37] Smolík J, Lazaridis M, Moravec P, Schwarz J, Zaripov SK, Ždímal V. Indoor aerosol particle deposition in an empty office. *Water Air Soil Poll* 2005;165:301-12.
- [38] Zhu Y, Hinds WC, Krudysz M, Kuhn T, Froines J, Sioutas C. Penetration of freeway ultrafine particles into indoor environments. *Atmos Environ* 2005;36:303-22.
- [39] Bennett DH, Koutrakis P. Determining the infiltration of outdoor particles in the indoor environment using a dynamic model. *J Aerosol Sci* 2006;37:766-85.
- [40] Rim D, Wallace L, Persily A. Infiltration of outdoor ultrafine particles into a test house. *Environ Sci Technol* 2010;44:5908-13.

- [41] Stephens B, Siegel JA. Penetration of ambient submicron particles into single-family residences and associations with building characteristics. *Indoor Air* 2012;22:501-13.
- [42] Atlas of the Prague Environment, [http://www.premis.cz/atlaszp/En\\_default.htm](http://www.premis.cz/atlaszp/En_default.htm), 2008 (accessed 02/04/10).
- [43] Andelová L, Smolík, J, Ondráčková L, Ondráček J, López-Aparicio S, Grøntoft T, et al. Characterization of airborne particles in the Baroque Library Hall in Prague. *e-Preservation Science* 2010;7:141-46.
- [44] Congrong H, Morawska L, Gilbert D. Particle deposition rates in residential houses. *Atmos Environ* 2005;39:3891-99.
- [45] D'Agostino D, Congedo PM. CDF modeling and moisture dynamics implications of ventilation scenarios in historical buildings. *Build Environ* 2014;79:181-93.
- [46] Camuffo D, Van Grieken R, Busse HJ, Sturaro G, Valentino A, Bernardi A, et al. Environmental monitoring in four European museums. *Atmos Environ* 2001;35:S127-40.
- [47] Hinds WC. *Aerosol Technology*. New York: John Wiley & Sons; 1999
- [48] Thornburg J, Ensor DS, Rodes CE, Lawless PA, Sparks LE, Mosley RB. Penetration of particles into buildings and associated physical factors. Part I: Model development and computer simulations. *Aerosol Sci Technol* 2001;34:284-96.
- [49] Worobiec A, Samek L, Karaszkiwicz P, Kontozova-Deutsch V, Stefaniak EA, Van Meel K, et al. A seasonal study of atmospheric conditions influenced by the intensive tourist flow in the Royal Museum of Wawel Castle in Cracow, Poland. *Microchem J* 2008;90:99-106.
- [50] Rim D, Persily A, Emmerich S, Stuart Dols W, Wallace L. Multi-zone modeling of size-resolved outdoor ultrafine particle entry into a test house. *Atmos Environ* 2013;69:219-30.
- [51] El Orch Z, Stephens B, Waring MS. Predictions and determinants of size-resolved particle infiltration factors in single-family homes in the U.S. *Build Environ* 2014;74:106-18.
- [52] Diapouli E, Chaloukakou A, Koutrakis P. Estimating the concentration of indoor particles of outdoor origin: A review. *J Air Waste Manage* 2013;63:1113-29.

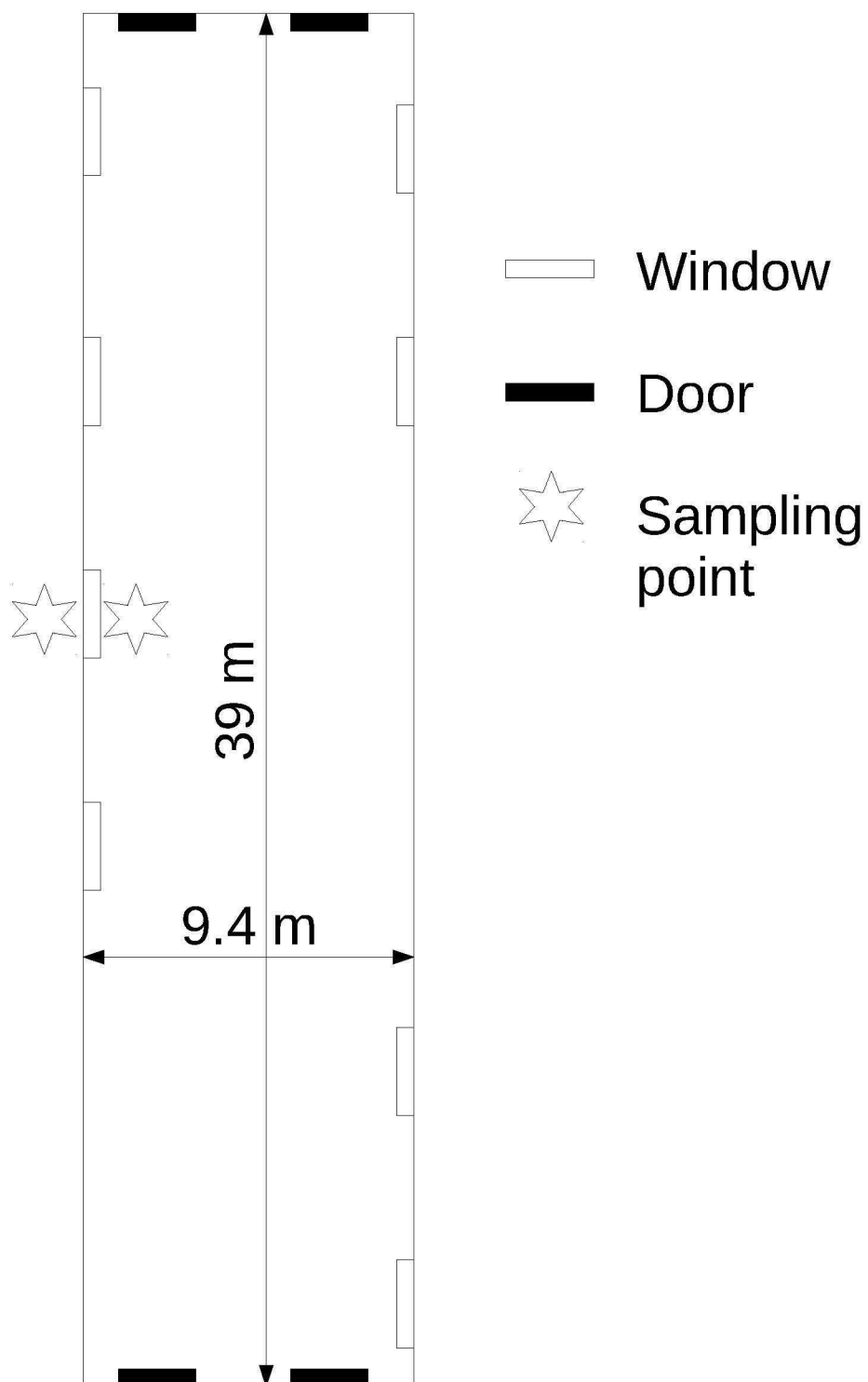
[53] Vette AF, Rea AW, Lawless PA, Rodes CE, Evans G, Highsmith VR, et al. Characterization of indoor-outdoor aerosol concentration relationships during the Fresno PM exposure studies. *Aerosol Sci Technol* 2001;34:118-26.

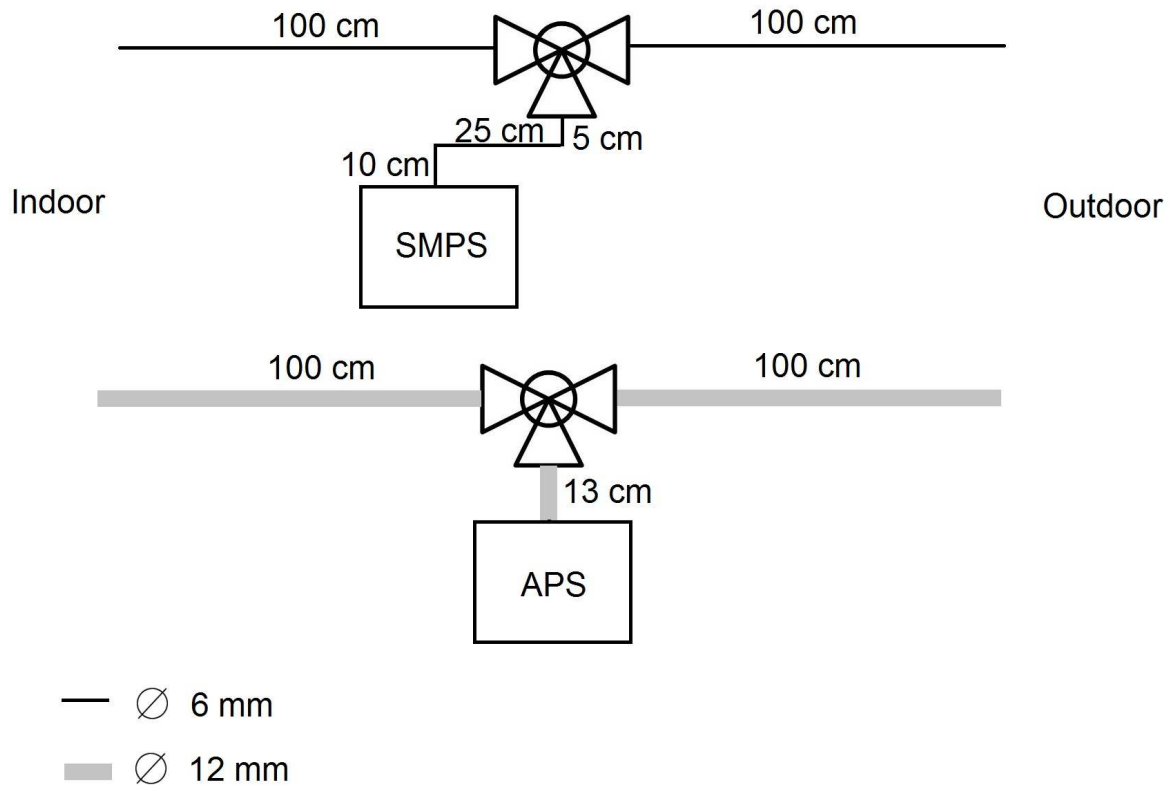
[54] Chen C, Zhao B, Zhou W, Jian X, Tan Z. A methodology for predicting particle penetration factor through cracks of windows and doors for actual engineering application. *Build Environ* 2012;47:339-48.

[55] Lai ACK. Particle deposition indoors: a review. *Indoor Air* 2002;12:211-14.

[56] Chao CYH, Wan MP, Cheng ECK. Penetration coefficient and deposition rate as a function of particle size in non-smoking naturally ventilated residences. *Atmos Environ* 2003;37:4233-41.

[57] Wallace LA, Emmerich SJ, Howard-Reed C. Effect of central fans and in-ducts filters on deposition rates of ultrafine and fine particles in an occupied townhouse. *Atmos Environ* 2004;38:405-13.





- Indoor/outdoor particle concentration was measured in a naturally ventilated building.
- A mass balance model was used to model indoor concentration.
- Deposition rate  $k$  and penetration efficiency  $P$  determined in 13 size intervals.
- Infiltration of outdoor particles and contribution from indoor sources was evaluated.
- Infiltration factor was in agreement with I/O ratio.

ACCEPTED MANUSCRIPT